remote sensing

MDPI

Editorial

Remote Sensing of Landslides—A Review

Chaoying Zhao [1] and Zhong Lu [2,*]

[1] School of Geology Engineering and Geomatics, Chang'an University, No. 126, Yanta Road, Xi'an 710054, China; cyzhao@chd.edu.cn
[2] Huffington Department of Earth Sciences, Southern Methodist University, P.O. Box 750395, Dallas, TX 75275, USA
* Correspondence: zhonglu@smu.edu

Received: 7 February 2018; Accepted: 8 February 2018; Published: 11 February 2018

Abstract: Triggered by earthquakes, rainfall, or anthropogenic activities, landslides represent widespread and problematic geohazards worldwide. In recent years, multiple remote sensing techniques, including synthetic aperture radar, optical, and light detection and ranging measurements from spaceborne, airborne, and ground-based platforms, have been widely applied for the analysis of landslide processes. Current techniques include landslide detection, inventory mapping, surface deformation monitoring, trigger factor analysis and mechanism inversion. In addition, landslide susceptibility modelling, hazard assessment, and risk evaluation can be further analyzed using a synergic fusion of multiple remote sensing data and other factors affecting landslides. We summarize the 19 articles collected in this special issue of *Remote Sensing of Landslide*, in the terms of data, methods and applications used in the papers.

Keywords: landslide; remote sensing; deformation; detection; susceptibility modelling

1. Introduction

Landslides are defined as the movement of a mass of rock, debris or earth down a slope, and can result in enormous casualties and huge economic losses. So great care has been taken to study landslide processes, including the type, location, stability, trigger factors, susceptibility and risk. Diverse remote sensing data have been well utilized, including spaceborne synthetic aperture radar (SAR) and optical remote sensing, airborne light detection and ranging (LiDAR), ground-based SAR and terrestrial LiDAR, incorporating in-situ surveying measurements and observations of environmental factors. Different techniques have been employed to generate landslide inventory maps, monitor landslide deformation, and model landslide susceptibility. Finally, multi-scale landslide spectra, including earth flow, collapse and cliff recession, ranging from a localized specific site to a large coverage catchment or basin in the spatial domain, from minutes to decades in the time domain, and from mm/year to tens of meters in the deformation magnitude over ten countries are presented in this special issue.

2. Data

2.1. SAR

Owing to their broad coverage and high spatial (and to some extent, temporal) resolution, and the ability to operate under all weather conditions, SAR data have been widely used in landslide research. Satellite SAR data used in this special issue include archived ERS and Envisat ASAR [1], ALOS/PALSAR [2,3], COSMO-SkyMed constellation [4], TerraSAR-X [5], TerraSAR-X/TanDEM-X [6], and Sentinel-1 [7]. In addition, "Envisat 2010+" data, which started on 22 October 2010 and lasted until the communication with the Envisat satellite was suddenly lost on 8 April 2012, were involved. The orbit of the Envisat satellite was lowered from about 800 km to about 783 km in order to conserve

fuel and extend its life [8]. Lastly, ground-based (GB) SAR data were undertaken to measure the rapid-moving earth flow [9].

2.2. Optical Remote Sensing

Optical remote sensing images were mainly applied to generate landslide inventory. Optical sensors involved in this special issue include long time-series of Landsat TM/ETM, SPOT 1-5, ASTER, IRS-1C LISS III, and RapidEye between 1986 and 2016 [10], ZY-3 satellite high spatial resolution satellite images [11], and GF-1 [12]. In addition, an image correlation algorithm was applied to SPOT-5 images to investigate the landslide cinematics [13].

2.3. LiDAR

Multi-temporal LiDAR images and ortho-photos were compared to quantify landscape changes caused by an active landslide [14]. The ground-based terrestrial laser scanner (TLS) LiDAR can produce highly detailed 3 dimensional (3D) images within minutes, allowing the study of 3D surface changes of landslides [15].

2.4. DEM

Digital elevation models (DEMs) were generated from Indian Remote Sensing Satellite (IRS) P5 images by stererophotogrammetry [16], and TerraSAR-X/TanDEM-X images by InSAR [6], respectively. Then, the DEM difference was used to quantify the erosion and cliff recession and to evaluate the landslide volume [16].

3. Method

3.1. Landslide Detection or Investigation

An object-oriented landslide mapping framework based on random forests and mathematical morphology from high spatial resolution optical satellite images was proposed to detect historically occurred landslides [11]. An automated detection algorithm was developed to recognize loess landslides by combining spectral, textural, and morphometric information with auxiliary topographic parameters based on high-resolution multispectral satellite data and high-precision DEM [12]. In addition, spatial autocorrelation changes induced by event landslides were measured in a set of multi-temporal Sentinel-1 intensity images [7]. Furthermore, potential landslides over large area were detected based on surface deformation maps from InSAR [2,8].

3.2. Landslide Monitoring

Time series surface deformation based on spaceborne satellite data are calculated with persistent scatterer interferometry (PSI) [1] and small baseline subset (SBAS) InSAR [2,3,8], as well as the integration of PS and Quasi-PS (QPS), which take advantage of two different image connection graphs in time-series InSAR processing [1]. The deformation retrieved from pre-installed corner reflectors imaged by X-band COSMO-SkyMed constellation SAR data can overcome the temporal decorrelation to obtain high-precision deformation results [16]. The combination of the dual-geometry InSAR datasets allowed the derivation of the vertical and the horizontal (east-west) components of the movement [1]. 3D surface changes can be monitored with TLS LiDAR and GNSS [15] or SAR intensity offset tracking method with a prior deformation model [5]. Finally, continuous fast-moving deformation of earth flow can be obtained by the GB-InSAR technique [9].

As for the large deformation field (~meters in magnitude), two image correlator software packages (MicMac and Cosi-Corr) were applied to high spatial resolution ortho-rectified SPOT-5 images, where image control points were selected by the scale invariant feature transform method [13]. Moreover, if the mass moved away or so-called erosion occurred, differential DEM technique based on TanDEM-X data could be used geomorphological changes in the catchment region [6]. Finally, the integrated

use of satellite, aerial, and drone images and ground-based GPS surveys allowed the mapping of the temporal evolution of a landslide system [1].

3.3. Landslide Susceptibility Modeling

Landslide susceptibility indicates how likely a landslide is to occur at a location with a certain combination of predisposing factor values. Bivariate and multivariate statistical techniques, through the use of Dempster-Shafer weights of evidence and multiple regression methods [17], and techniques that combine principle component analysis and fuzzy membership techniques were used and tested [18]. A physically based model was applied in the rainfall-induced shallow landslide susceptibility analysis because of its ability to reproduce the physical processes governing landslide occurrence [19]. In addition, landslide activity was assessed by the means of an activity matrix derived from InSAR measurements from descending and ascending passes [1].

4. Experiments

The landslide processes for typical landslides, including earth flow, collapse and cliff recession over ten countries, are collected in this special issue (Figure 1). Multi-scale landslide spectra ranging from a small specific site to a large coverage catchment or basin in the spatial domain, from minutes to decades in the time domain, and from mm/year to tens of meters in deformation magnitude are all presented.

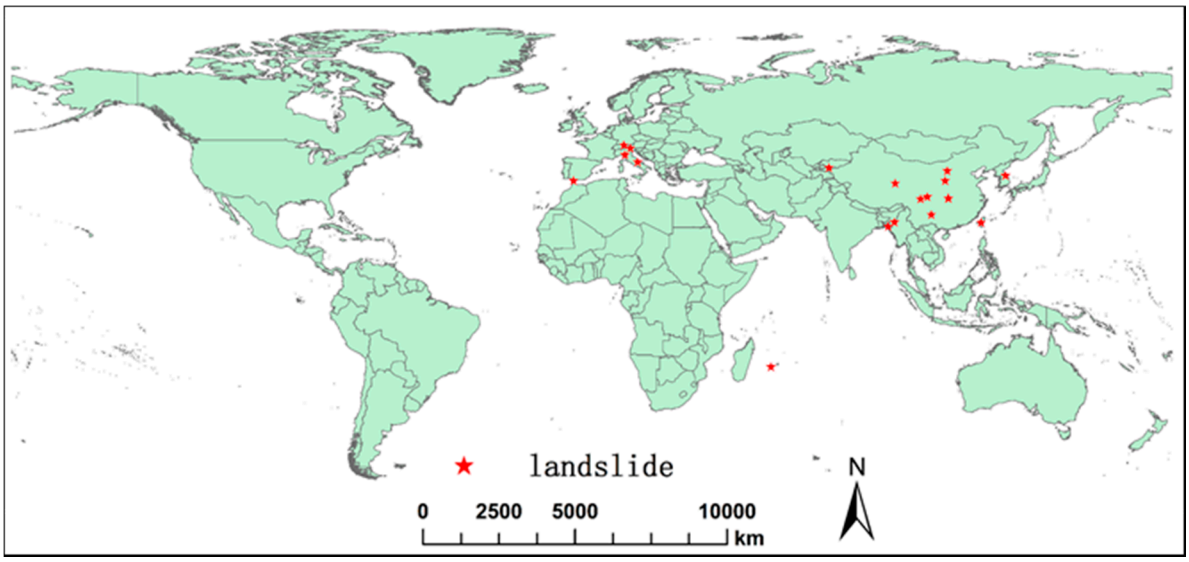

Figure 1. The distribution of landslides over ten countries in the special issue.

4.1. Landslides Detection

Twelve landslides in Guanling, Guizhou, China were detected with ALOS/PALSAR InSAR. The mapped landslides show high consistency with results from optical images [2]. An extensive investigation of more than 90 landslides affecting a small river basin in Central Italy was performed by combining field surveys and remote sensing techniques [1]. An event landslide in Chin Division, Myanmar was detected from 16 Sentinel-1A SAR images; pixel-based changes between consecutive SAR intensity images were obtained from the log-ratio index [7]. High spatial resolution satellite images from 'ZY-3' were utilized to identify the landslides over the Three Gorges Reservoir area of Yangtze River, China [11]; results indicated that the combination of random forests and mathematical morphology operations provided the best model for landslide mapping.

4.2. Landslide Deformation Monitoring

A pre-slide time-series deformation was monitored with SBAS InSAR technique over the Guanling landslide occurred on 28 June 2010 [2]. A complex earthflow with spatially varying displacement patterns over Corvara landslides in the Italian Alps was assessed using 16 artificial corner reflectors installed on the source, track and accumulation zones of the landslide, based on multi-temporal X-band COSMO-SkyMed constellation imagery [4]. The satellite observations were validated by differential GPS time-series data and proved to be a promising method for monitoring landslides characterized by linear and relatively slow movement rates [4]. GB-InSAR was applied to track the rapid movement of earth flows over the Capriglio landslide in northern Appennines, Italy, which was re-activated in April 2013 [9]. The authors demonstrated the capability of GB-InSAR in measuring high deformation rates (~meters/days) to support local authorities in hazard assessment and risk management. Recent landslide movements in Tsaoling, Taiwan were tracked by analyzing DEM time series reconstructed from TerraSAR-X/TanDEM-X image pairs [6]. Results showed that multi-temporal high-resolution DEMs can assess the change in recession rate and other geomorphological modifications caused by landslides [6]. The cinematics of "Mare à Poule d'Eau" landslide (Réunion, France) were measured with SPOT-5 images; the shift of the landslide for the 2006–2008 period reached 8.5 m, but the dispersion of the results was high [13]. In Arcos de la Frontera, Spain, "ENVISAT 2010+" project was aimed to monitor surface displacement for the period spanning April 2011–January 2012 with the SBAS InSAR method; the standard deviation of the accumulated LOS displacement reached 5.5 mm [8].

4.3. Landslide Trigger Factor Analysis

Landslides are mainly triggered by natural factors, such as the 2008 Wenchuan earthquake, China [16], freeze/thaw in the Qinghai-Tibet engineering corridor [15], and heavy rainfalls in different regions reported in this special issue [2,3,8,9,17,19]. On the other hand, landslides can also be caused by anthropogenic activities, including rapid urbanization through hill-cutting in densely populated Bangladesh [17], impoundment of the reservoir in the Three Gorges Reservoir of the Yangtze River, China [11], under-construction of the reservoir in the eastern Qinghai-Tibet plateau in the southwestern part of China [3], and underground mining in the northern Shaanxi province, China [5].

4.4. Landslide Susceptibility Modelling

Landslide susceptibility maps in Chittagong City Corporation, Bangladesh were developed through the use of Dempster-Shafer weights of evidence and multiple regression methods [17]. Multi-temporal assessment of the state of landslide activity was performed based on geomorphological evidence criteria and past ground displacement measurements obtained by InSAR in the basin of Abruzzi, Italy [1]. Landslide susceptibility mapping was presented by integrating information theory, K-means cluster analysis and statistical models in the Three Gorges Area, China [18]. The regional landslide susceptibility and uncertainty assessment in Gangwon Province, Republic of Korea was obtained by fuzzy set theory coupled with the vertex and the point estimate methods [19].

4.5. Landslide Mechanism Inversion

In situ and remote sensing techniques, along with detailed geological information and urban damage distribution, were used to interpret the mechanism of landslides in Arcos de la Frontera, Spain [8]. The combination of ascending and descending InSAR results better defined the type of movement and the mechanism of the investigated landslides in central Italy [1]. InSAR deformation, along with borehole logs and the knowledge of the regional geological background, were used to explain the mechanism and formation of an ancient deep-seated translational landslide in the eastern Qinghai-Tibet plateau [3]. In the Qinghai-Tibet engineering corridor, the seasonal subsidence was caused by thaw settlement, while the seasonal uplift trend was probably due to frost heaving [15].

Lastly, the failure of the Guanling landslide was caused by the shear in the locking segment and the main trigger for the shear was heavy rainfall [2].

5. Conclusions and Perspectives

Landslides can be triggered by a number of mechanisms, including intense or long-duration rainstorms, earthquakes, permafrost degradation, reservoir impoundment, and urbanization, among others. Papers in this special issue have clearly demonstrated that mapping landslide deformation and activity is fundamental for the assessment and reduction of landslide hazards and risks. Multiple remote sensing techniques, including SAR, optical, LiDAR, ortho-photo, and DEM obtained from spaceborne, airborne, and ground-based platforms, can be utilized to monitor landslide processes. Landslide mechanism and susceptibility mapping can be further analyzed using a synergic fusion of multiple remote sensing data, numerical models, and other factors affecting landslides. With the increase in temporal and spatial resolution, remote sensing imagery will play a more important role in landslide monitoring, hazard assessment, and risk evaluation.

Acknowledgments: This research is funded by Natural Science Foundation of China (Grant No. 41628401, and 41731066) and supported by China 111 Plan (Grant No. B18046) and the Shuler-Foscue Endowment at Southern Methodist University.

Conflicts of Interest: The authors declare no conflicts of interest.

References

1. Bozzano, F.; Mazzanti, P.; Perissin, D.; Rocca, A.; Pari, P.; Discenza, M. Basin Scale Assessment of Landslides Geomorphological Setting by Advanced InSAR Analysis. *Remote Sens.* **2017**, *9*, 267. [CrossRef]
2. Kang, Y.; Zhao, C.; Zhang, Q.; Lu, Z.; Li, B. Application of InSAR Techniques to an Analysis of the Guanling Landslide. *Remote Sens.* **2017**, *9*, 1046. [CrossRef]
3. Qi, S.; Zou, Y.; Wu, F.; Yan, C.; Fan, J.; Zang, M.; Zhang, S.; Wang, R. A Recognition and Geological Model of a Deep-Seated Ancient Landslide at a Reservoir under Construction. *Remote Sens.* **2017**, *9*, 383. [CrossRef]
4. Schlögel, R.; Thiebes, B.; Mulas, M.; Cuozzo, G.; Notarnicola, C.; Schneiderbauer, S.; Crespi, M.; Mazzoni, A.; Mair, V.; Corsini, A. Multi-Temporal X-Band Radar Interferometry Using Corner Reflectors: Application and Validation at the Corvara Landslide (Dolomites, Italy). *Remote Sens.* **2017**, *9*, 739. [CrossRef]
5. Yang, Z.; Li, Z.; Zhu, J.; Preusse, A.; Yi, H.; Hu, J.; Feng, G.; Papst, M. Retrieving 3-D Large Displacements of Mining Areas from a Single Amplitude Pair of SAR Using Offset Tracking. *Remote Sens.* **2017**, *9*, 338. [CrossRef]
6. Du, Y.; Xu, Q.; Zhang, L.; Feng, G.; Li, Z.; Chen, R.; Lin, C. Recent landslide movement in Tsaoling, Taiwan tracked by TerraSAR-X/TanDEM-X DEM time series. *Remote Sens.* **2017**, *9*, 353. [CrossRef]
7. Mondini, A. Measures of Spatial Autocorrelation Changes in Multitemporal SAR Images for Event Landslides Detection. *Remote Sens.* **2017**, *9*, 554. [CrossRef]
8. Bru, G.; González, P.J.; Mateos, R.M.; Roldán, F.; Herrera, G.; Béjar-Pizarro, M.; Fernández, J. A-DInSAR Monitoring of Landslide and Subsidence Activity: A Case of Urban Damage in Arcos de la Frontera, Spain. *Remote Sens.* **2017**, *9*, 787. [CrossRef]
9. Bardi, F.; Raspini, F.; Frodella, W.; Lombardi, L.; Nocentini, M.; Gigli, G.; Morelli, S.; Corsini, A.; Casagli, N. Monitoring the Rapid-Moving Reactivation of Earth Flows by Means of GB-InSAR: The April 2013 Capriglio Landslide (Northern Appennines, Italy). *Remote Sens.* **2017**, *9*, 165. [CrossRef]
10. Golovko, D.; Roessner, S.; Behling, R.; Wetzel, H.; Kleinschmit, B. Evaluation of Remote-Sensing-Based Landslide Inventories for Hazard Assessment in Southern Kyrgyzstan. *Remote Sens.* **2017**, *9*, 943. [CrossRef]
11. Chen, T.; Trinder, J.C.; Niu, R. Object-Oriented Landslide Mapping Using ZY-3 Satellite Imagery, Random Forest and Mathematical Morphology, for the Three-Gorges Reservoir, China. *Remote Sens.* **2017**, *9*, 333. [CrossRef]
12. Sun, W.; Tian, Y.; Mu, X.; Zhai, J.; Gao, P.; Zhao, G. Loess Landslide Inventory Map Based on GF-1 Satellite Imagery. *Remote Sens.* **2017**, *9*, 314. [CrossRef]

13. Bivic, R.L.; Allemand, P.; Quiquerez, A.; Delacourt, C. Potential and Limitation of SPOT-5 Ortho-Image Correlation to Investigate the Cinematics of Landslides: The Example of "Mare à Poule d'Eau" (Réunion, France). *Remote Sens.* **2017**, *9*, 106. [CrossRef]
14. Kamps, M.; Bouten, W.; Seijmonsbergen, A. LiDAR and Orthophoto Synergy to optimize Object-Based Landscape Change: Analysis of an Active Landslide. *Remote Sens.* **2017**, *9*, 805. [CrossRef]
15. Luo, L.; Ma, W.; Zhang, Z.; Zhuang, Y.; Zhang, Y.; Yang, J.; Cao, X.; Liang, S.; Mu, Y. Freeze/Thaw-Induced Deformation Monitoring and Assessment of the Slope in Permafrost Based on Terrestrial Laser Scanner and GNSS. *Remote Sens.* **2017**, *9*, 198. [CrossRef]
16. Ren, Z.; Zhang, Z.; Yin, J. Erosion Associated with Seismically-Induced Landslides in the Middle Longmen Shan Region, Eastern Tibetan Plateau, China. *Remote Sens.* **2017**, *9*, 864. [CrossRef]
17. Ahmed, B.; Dewan, A. Application of Bivariate and Multivariate Statistical Techniques in Landslide Susceptibility Modeling in Chittagong City Corporation, Bangladesh. *Remote Sens.* **2017**, *9*, 304. [CrossRef]
18. Wang, Q.; Wang, Y.; Niu, R.; Peng, L. Integration of Information Theory, K-Means Cluster Analysis and the Logistic Regression Model for Landslide Susceptibility Mapping in the Three Gorges Area, China. *Remote Sens.* **2017**, *9*, 938. [CrossRef]
19. Park, H.J.; Jang, J.Y.; Lee, J.H. Physically Based Susceptibility Assessment of Rainfall-Induced Shallow Landslides Using a Fuzzy Point Estimate Method. *Remote Sens.* **2017**, *9*, 487. [CrossRef]